



Contents lists available at ScienceDirect

Nuclear Inst. and Methods in Physics Research, A

journal homepage: www.elsevier.com/locate/nima

Beam energy measurement on LINAC-200 accelerator and energy calibration of scintillation detectors by electrons in range from 1 MeV to 25 MeV



M. Krmar^{a,*}, Y. Teterev^b, A.G. Belov^b, S. Mitrofanov^b, S. Abou El-Azm^c, M. Gostkin^c, V. Kobets^c, U. Kruchonak^c, A. Nozdrin^c, S. Porokhovoy^c, M. Demichev^c

^a Physics Department, Faculty of Sciences, University of Novi Sad, Novi Sad, Serbia

^b JINR, Flerov Laboratory of Nuclear Reactions, Dubna, Russia

^c JINR, Dzhelapov Laboratory of Nuclear Problems, Dubna, Russia

ARTICLE INFO

Keywords:

Energy calibration

BGO

LaBr:Ce and plastic scintillation detectors

Bremsstrahlung

Photoactivation

Gamma spectroscopy

ABSTRACT

Accurate determination of the energy of LINAC-200 fast electrons was performed using several photonuclear reactions carried out on natural Indium after conversion of electron energy in bremsstrahlung in thick Tungsten target. Natural Indium was used as an activation detector and the ratios of saturation activities $R(^{113m}\text{In})/R(^{115m}\text{In})$, $R(^{114m}\text{In})/R(^{115m}\text{In})$ and $R(^{111}\text{In})/R(^{115m}\text{In})$ were used as a measure of the endpoint energy of the bremsstrahlung beam (and energy of electrons striking the bremsstrahlung target as well). Energy dependence of the three ratios of saturation activities were determined by using the bremsstrahlung produced by electrons accelerated by Microtron to the energies known with accuracy not worse than 0.1 MeV. Three types of scintillation detectors (LaBr3:Ce, BGO and plastic) were calibrated using electrons having energies from 1.17 MeV to 25 MeV. In low energy region photoelectrons produced by ^{60}Co gamma radiation in the detector itself were used, as well as high energy electrons (from 11 MeV to 25 MeV) accelerated by LINAC-200.

1. Introduction

The necessary condition for the progress in nuclear physics and in the high energy physics is the development of the new types of detector systems that become increasingly complex over time. One of the most important tasks in the design of new experimental infrastructure is to provide detectors able to function in high load conditions with high reliability and accuracy. The development of new detectors is also important for different applications, based, for example, on the use of synchrotron radiation sources or intensive X-ray machines as therapy accelerators. JINR has been facing several challenges lately. One of them is related to the development of the research program on the XFEL (X-ray Free Electron Laser) complex [1]. JINR member countries are involved in the creation of experimental stations based on detectors with high spatial and energy resolution. Future experiments on NICA collider [2] could be required the development of a big calorimeter, which includes a number of detectors, among which are detectors of high energy electrons. An integral part of several designed detectors may be LaBr3:Ce (LaBr in further text), BGO and plastic scintillators. This means that it is essential to know the response of LaBr, BGO and plastic detectors for various types of incident particles, including electrons.

Energy calibration of BGO detectors in the MeV region of gamma energies is described in publications [3–5]. It was obtained [4] that

the energy calibration of BGO detectors is linear in the energy region from 0.662 MeV (^{137}Cs) to 20.43 MeV ($^{11}\text{B}(p, \gamma)^{12}\text{C}$ reaction). Plastic scintillators are frequently used in very different experimental setups and have a good linearity for MeV region electrons [6,7]. Thanks to its excellent properties, novel LaBr detectors have awakened the very curiosity, especially in the field of detection of high-energy gamma radiation [8,9]. The most important advantages of LaBr detectors (high light yield and sub nano-second decay time of scintillation light) have led to the non linearity in energy response, mostly due to large PMT currents. Non-linear energy calibration of LaBr detectors is analyzed in several references [10,11]. This problem can be solved by the reduction of PMT voltage, by taking signal from one of the dynodes or even by inserting a filter between LaBr crystal and photo-cathode to attenuate the light [8,12,13]. In this case, some kind of trade of between linearity and energy resolution should be done.

The ability to study the characteristics of prototype detectors depends, to a large extent, on the availability of the test beam. The characteristics of this test beam should be well known. JINR is in possession of a linear accelerator LINAC-200 whose first section can provide electrons in the energy range from 10 MeV to 25 MeV. The simplest method to determine the beam energy is to use the known magnetic field strength in the beam-out dipole magnet. However, this

* Corresponding author.

E-mail address: krmar@df.uns.ac.rs (M. Krmar).

<https://doi.org/10.1016/j.nima.2019.04.104>

Received 18 March 2019; Received in revised form 24 April 2019; Accepted 28 April 2019

Available online 8 May 2019

0168-9002/© 2019 Elsevier B.V. All rights reserved.

method depends on thorough magnet calibration including the measurement of the field map for various current values and careful study of the hysteresis. That is why an independent reliable method to determine the beam energy at certain reference points would be very valuable.

It is shown in a recent publication [14] that the ratios of saturation activities of several products of photonuclear reactions, performed on natural Indium, can be a sensitive test of endpoint energy of bremsstrahlung. Ratios of saturation activities of several products of photonuclear reactions obtained after exposition of In foils to photon beam of Microtron MT25 were determined in the broad region of bremsstrahlung endpoint energies. The reason why a cyclic accelerator MT25 was chosen to be a reference machine is that the energy of its electrons is known with accuracy not worse than 0.1 MeV [15]. In the next step, irradiation of the same In activation detectors in photon beam of LINAC-200 was done. It is very important to underline that the photon beam of LINAC-200 was produced in the Tungsten target of Microtron. The obtained ratios of saturation activities were used to estimate the energy of LINAC-200 accelerator by comparison with Microtron derived ones.

There were two objectives of the research described in this paper: (i) to apply a new method for estimating the energy of accelerated electrons using photonuclear reactions performed in two bremsstrahlung beams - Microtron (having a well calibrated output, including reliable data of electron energies) and LINAC which should be calibrated; (ii) to calibrate LaBr, BGO and plastic detectors in the broad region of electron energies, up to 25 MeV.

2. Materials and methods

The yield of some nuclear reaction is usually described by the quantity called saturation activity R :

$$R = \int_{E_{th}}^{E_{max}} \sigma(E) \cdot \Phi(E) \cdot dE \quad (1)$$

where $\sigma(E)$ is cross section for observed nuclear reaction, $\Phi(E)$ is the flux of incident particles (in our case photons), E_{th} is the energy threshold for the nuclear reaction and E_{max} is the maximal energy of particles. If the bremsstrahlung is used, E_{max} corresponds to the energy of electrons striking the target. Saturation activity can be experimentally determined using the intensity of a single gamma line in recorded gamma spectra as:

$$R = \frac{N_\gamma \lambda M}{m N_{Av} \varepsilon \eta p_\gamma e^{-\lambda \Delta t} (1 - e^{-\lambda t_{irr}}) (1 - e^{-\lambda t_m})} \quad (2)$$

where N_γ is the number of detected gamma photons of chosen energy, λ is the decay constant, M and m are the mass number and the mass of the activation detector used, N_{Av} is Avogadro number, ε is the absolute efficiency of the detector at the energy of observed gamma line, η is the natural abundance of activated isotope, p_γ is the quantum yield of detected photons, Δt , t_{irr} and t_m are cooling, irradiation and measurement time respectively.

It is shown in a recent publication [14] that the ratio of saturation activities of two products of photonuclear reactions is a function of E_{max} . It is a consequence of the fact that the energy dependences of the cross sections for different photonuclear reactions can differ significantly. Natural Indium, having two isotopes (^{113}In (4.25% in natural metal) and ^{115}In (95.75%)), in the form of tiny disks (20 mm diameter, 0.215 g cm^{-2}) was chosen to be the activation detector because several photonuclear reactions can be followed simultaneously. Four photonuclear reactions, depicted in Table 1 were used in this study.

In order to obtain the dependence of the saturation activities (and their ratio) from the maximal photon energy E_{max} , the irradiation of the In targets in the photon beam of Microtron was performed in the energy range from 10 to 23 MeV. The exposure time was from 2 min at 23 MeV

Table 1

Data relevant to the nuclear reactions being monitored. $T_{1/2}$ is half-life of reaction product and E_γ and p_γ are energies of the measured gamma radiation and quantum yields respectively.

Photonuclear reaction	$T_{1/2}$ of reaction product	E_γ [keV] (p_γ)
$^{115}\text{In}(\gamma, \gamma')^{115\text{m}}\text{In}$	4.486 h	336.26 (0.458)
$^{115}\text{In}(\gamma, n)^{114\text{m}}\text{In}$	49,51 d	190.29 (0.156)
$^{115}\text{In}(\gamma, 2n)^{113\text{m}}\text{In}$	1.658 h	391.69 (0.642)
$^{113}\text{In}(\gamma, 2n)^{111}\text{In}$	2.81 d	245,4(0,94)

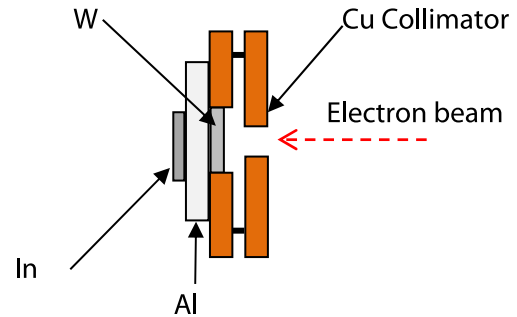


Fig. 1. Bremsstrahlung target used in experiment.

to 30 min at 10 MeV. Electron current of Microtron was changed in this experiment to get satisfactorily high activities of reaction products. For example, the electron current was 1.5 μA at 23 MeV and 10 μA at 10 MeV.

A practically mono-energetic electron beam of the frequency 25 Hz and the pulse duration is 2 μs from LINAC-200 is delivered with different energies (after calibration it was confirmed that the energy interval was from 11 MeV to 24 MeV). It was estimated that a 45° deflection in magnetic field provides a part of electron energy spectra with a resolution about ± 200 keV. A bremsstrahlung target, taken from Microtron was placed in order to do the exposure of the In activation detectors in the photon beam. As presented in Fig. 1, the electron beam is focused into a 12 mm Cu collimator. The bremsstrahlung target was made in the form of a tungsten disk 3.3 mm thick. A 20 mm thick Al disk was located behind the target in order to absorb electrons that had passed through the tungsten target. The additional function of the collimator was to monitor efficiency of the electron beam focusing on the target. Indium activation detectors were placed at a distance of 7 cm from exit window of electrons. In this experiment the beam intensities between 20 nA and 80 nA were set depending on beam energy. The irradiation time varied from 30 min to 130 min.

In order to measure the electron spectra from LINAC accelerator, three scintillation detectors, based on $\text{LaBr}_3:\text{Ce}$ [16], BGO [5] crystals and a plastic scintillator (polystyrene + PTP + POPOP) [17] were chosen. Detectors have a cylindrical shape with the following dimensions: 76 mm diameter and 65 mm height for BGO, 50.8 mm \times 50.8 mm for LaBr and 100 mm \times 400 mm for plastic. The ^{60}Co gamma source was chosen to provide the calibration in the low energy region, up to 2.5 MeV. It should be noted that in the case of the plastic scintillator in the low energy range, the Compton edge recorded in gamma spectrum of ^{137}Cs and ^{60}Co was used instead of ^{60}Co full absorption peaks.

Detectors were placed in the electron beam and the spectra were recorded. The dimensions of LINAC-200 exit beam were 10×10 mm, bunch duration was 2 μs and frequency was 25 Hz. While Indium activation detectors were exposed to the beam of maximal intensity, during exposition of scintillation detectors the beam current was reduced to avoid the summing effect due to high counting rate. It is important that the time interval between electron entries in the scintillation crystal in bunch is greater than the time resolution of the detector. Such a low level of electron current is not possible to get on Microtron. For this reason LINAC-200 was chosen to be used in energy calibration of scintillation detectors.

Each scintillator has been connected to its own respective Hamamatsu PMT. Obtained PMT signals were digitized by an oscilloscope DRS-4 evaluation board, which have a 350 MHz input analog bandwidth and can digitize the signal with rate up to 5 Gigasamples per second. For LaBr and plastic scintillators 6 dB attenuator was used in order to reduce the signal amplitude below the 1 V limit. Chosen PMT voltages were 1400 V for plastic (3" R6091 PMT), 630 V for LaBr (2" R6231) and 1110 V for BGO (3" R6233) detectors. DRS-4 operated in self-triggering mode with trigger thresholds chosen in the range of 2–90 mV depending on PMT signal level.

Offline integration of digitized signal over an automatically determined baseline level was done to obtain integrated charge. It was considered that this integral should be proportional to the energy deposited by incident particle in the bulk material of the detector. Integration time window was chosen to be 100 ns for LaBr and plastic and 400 ns for BGO because the latter has a longer scintillation time. The integrals of the signals obtained by the detection of the ^{60}Co gamma photons, as well as in the summing events of both ^{60}Co energies were used to obtain the relationship between gamma rays energy and integral values. The linear dependence between the energy and integral was extrapolated to higher energies, up to 25 MeV. Although it may be aware of the disadvantages of such an extrapolation, the obtained linear dependence was used as initial and preliminary calibration.

3. Measurements and results

Indium foils exposed in Microtron bremsstrahlung beam were measured by HPGe detector having relative efficiency of 25%. The detector was shielded by 5 cm of lead. All activation detectors were located directly on the vertical dipstick of the detector. Each of the In foils were measured two times. First spectra were used to determine the intensities of gamma lines emitted by short living products of reactions ($^{115\text{m}}\text{In}$ and $^{113\text{m}}\text{In}$). Cooling time for the first measurement was between 54 min and 220 min. A large counting rate and a dead time of the detector system, originating from shorter living products of reactions, were avoided by this way. The second measurements of irradiated In foils were performed the next day, after 20 h. In this measurement, weak gamma lines of long living reaction products $^{114\text{m}}\text{In}$ and ^{111}In , superimposed over a Compton continuum produced by high energy gamma lines of short living reaction product, can be determined with lower statistical uncertainty. The measurement time was 20 min for all In samples, except for the one exposed in the 10 MeV photon beam. In this case, both spectra were recorded for 30 min. Intensities of characteristic gamma lines (presented in Table 1) were determined and saturation activities were calculated using Eq. (2). Based on the obtained spectroscopic data, it was possible to calculate three different ratios of saturation activity $R(^{113\text{m}}\text{In})/R(^{115\text{m}}\text{In})$, $R(^{114\text{m}}\text{In})/R(^{115\text{m}}\text{In})$ and $R(^{111}\text{In})/R(^{115\text{m}}\text{In})$. This was done for several chosen endpoint energies of bremsstrahlung radiation. The obtained values were used to construct some kind of "calibration graphs" (presented in Fig. 2). The calibration graphs depict energy dependence of $R(^{111}\text{In})/R(^{115\text{m}}\text{In})$ and $R(^{113\text{m}}\text{In})/R(^{115\text{m}}\text{In})$ ratios of saturation activities. The $R(^{114\text{m}}\text{In})/R(^{115\text{m}}\text{In})$ ratio has an order of magnitude higher values and it is presented in Fig. 3. In both graphs, lines connecting experimentally derived points are drawn to guide the eye.

An identical measurement procedure was used after the irradiation of In foils in bremsstrahlung beam of LINAC-200 and the same ratios of saturation activities were calculated for two unknown energies. The first task was to check whether consistent estimates of unknown energy can be obtained by using the energy dependence of three different ratios of saturation activities. The result of this test is shown in Figs. 2 and 3. Horizontal lines denote the values of ratios of saturation activities calculated using the intensities of the gamma lines obtained after activation of the In foil in the photon beam of LINAC-200. The value of electron energy can be read as the abscissa of the crossing point of the horizontal line and the calibration curve, or more accurate, to fit

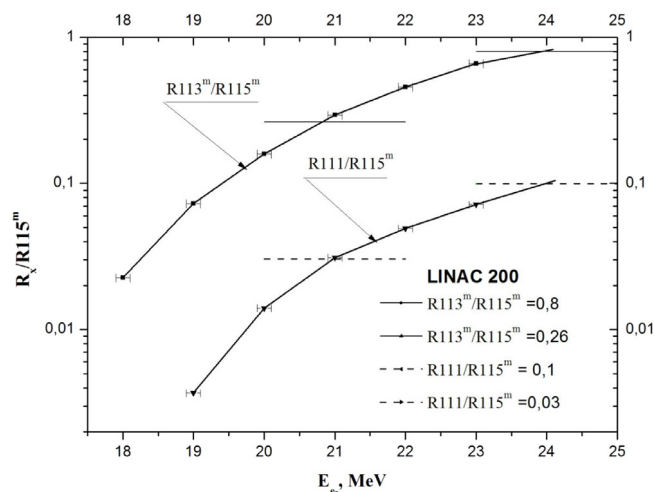


Fig. 2. Two LINAC photon beam energies read from the calibration curves obtained by the ratio of different isotopes of indium on the Microtron.

experimental points to some chosen function, and calculate the abscissa of the crossing point.

A second order polynomial function was good enough to fit points presented in Fig. 2. To fit data presented in Fig. 3 a sigmoid function was used.

It turned out that the first unknown energy of LINAC 200 was in the range of the measured points. It was obtained that the values of calculated ratios of saturation activities are $R(^{111}\text{In})/R(^{115\text{m}}\text{In}) = 0.030(1)$, $R(^{113\text{m}}\text{In})/R(^{115\text{m}}\text{In}) = 0.264(8)$ and $R(^{114\text{m}}\text{In})/R(^{115\text{m}}\text{In}) = 28.5(7)$. Using these values of ratios of saturation activities, it was obtained that the unknown energy of LINAC 200 is 20.8 MeV (from $R(^{114\text{m}}\text{In})/R(^{115\text{m}}\text{In})$ ratio), 20.8 MeV (from $R(^{113\text{m}}\text{In})/R(^{115\text{m}}\text{In})$ ratio) and 20.9 MeV (from $R(^{111}\text{In})/R(^{115\text{m}}\text{In})$ ratio). It was estimated that the experimental uncertainty of the estimated electron energy is about 0.2 MeV (1σ confidence level).

The second unknown LINAC 200 energy was slightly over range of the used Microtron energies, so estimation was done by extrapolation using obtained parameters of fit. The obtained ratios of saturation activities were $R(^{111}\text{In})/R(^{115\text{m}}\text{In}) = 0.099(3)$, $R(^{113\text{m}}\text{In})/R(^{115\text{m}}\text{In}) = 0.80(1)$ and $R(^{114\text{m}}\text{In})/R(^{115\text{m}}\text{In}) = 32.6(9)$. The estimated energies of LINAC 200 in this case were: 24.3 MeV (from $R(^{114\text{m}}\text{In})/R(^{115\text{m}}\text{In})$ ratio), 23.6 MeV (from $R(^{113\text{m}}\text{In})/R(^{115\text{m}}\text{In})$ ratio) and 24.0 MeV (from $R(^{111}\text{In})/R(^{115\text{m}}\text{In})$ ratio). Considering that the experimental uncertainty is about 0.2 MeV, it can be seen that the values obtained by extrapolation, although very close, do not overlap in the frame of 1σ interval.

Since three different ratios of saturation activities give consistent estimates of unknown energy, the $R(^{114\text{m}}\text{In})/R(^{115\text{m}}\text{In})$ ratio was used to calibrate LINAC-200. The main reason is the fact that nuclear reactions $^{115}\text{In}(\gamma, 2n)^{113\text{m}}\text{In}$ and $^{113}\text{In}(\gamma, 2n)^{111}\text{In}$ have a high threshold and cannot be used on energies below 17 MeV. Five different accelerating potentials of the LINAC-200 were chosen and Indium foils were activated in the bremsstrahlung beam. After the gamma spectroscopic measurements, the ratios of saturation activity $R(^{114\text{m}}\text{In})/R(^{115\text{m}}\text{In})$ were calculated and compared with the results obtained in the photon beam of Microtron. The achieved results are shown in Fig. 3. As explained in the previous case, the horizontal lines represent $R(^{114\text{m}}\text{In})/R(^{115\text{m}}\text{In})$ ratio measured after the exposition of activation detectors in LINAC-200 beam and the increasing line connects (just to guide the eye) $R(^{114\text{m}}\text{In})/R(^{115\text{m}}\text{In})$ values obtained after activation of In foils in Microtron photon beam.

Using the presented values of the $R(^{114\text{m}}\text{In})/R(^{115\text{m}}\text{In})$ ratio and parameters of the sigmoidal function obtained by the fit, energies of LINAC 200 were calculated. It was obtained that the endpoint energy

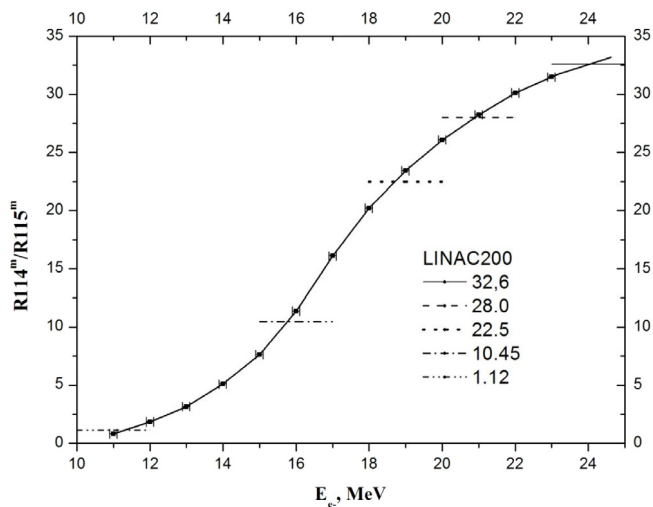


Fig. 3. Ratio of the saturation activities $R(^{114m}\text{In})/R(^{115m}\text{In})$ measured in Microtron and LINAC-200 photon beams.

of bremsstrahlung beams of LINAC-200 were 11.3 MeV, 15.8 MeV, 18.7 MeV, 20.9 MeV and 23.8 MeV.

After activation of the In foil, the bremsstrahlung target was removed and scintillation detectors were positioned in the electron beam. The spectra recorded in Co-60 gamma-source, 18.7 MeV (Plastic and LaBr) and 15.8 MeV (BGO) electron beam are depicted in Figs. 4 and 5.

In the range of 0–2.5 MeV, γ -sources were used for calibration as described in previous section. The best energy resolution has the LaBr, where both peaks of ^{60}Co (1.17 MeV and 1.33 MeV) are well separated (Fig. 4). It was determined that the energy resolution is 6% for LaBr in the LINAC vicinity, because of two reasons: noise due to accelerator operation and decreasing the HV to 630 V in order to reduce the PMT signal to fit the dynamic range and to reduce the non-linearity response. For optimum applied HV (900V) at the laboratory conditions, the resolution 2.3% was obtained, consistent with [10,11], although small nonlinearity was observed at 2.5 MeV sum gamma line. For BGO the resolution is 10% and near 30% for plastic in 1 MeV energy region. The energy resolution of plastic detectors should be treated as a rough estimation because of the high probability of Compton interactions in low Z materials and low probability of photopeak production. In the high energy region, 10 MeV–25 MeV, electron spectra in LINAC beam were recorded. The energy resolution for electrons in this energy range is about 5% for BGO, 8% for LaBr and 7% for plastic detectors. Structure of all electron peaks is similar, as can be seen in Figs. 4 and 5.

According to ESTAR NIST tables [18] all three scintillation detectors used in this experiment have the dimensions larger than the range of accelerated electrons. For example, ranges of 20 MeV electrons are 1.35 cm, 1.84 cm and 9.72 cm for BGO, LaBr and plastic respectively. Despite this fact, only a part of electrons will deposit full energy to the detector. Some portion of electron energy can escape detection through the emission of bremsstrahlung or annihilation radiation after e–p pair production. A radiation yield (fraction of kinetic energy of primary electron converted in bremsstrahlung) when 20 MeV electrons are passing through BGO, LaBr and Plastic are 0.3849, 0.3248 and 0.0707 respectively [18].

As can be seen, due to the low Z, the significantly lower portion of electron energy is converted in bremsstrahlung in plastic than in BGO or LaBr. This is a reason why the number of events in plastic peak is higher than in BGO and LaBr peaks under the same experimental conditions, as can be seen in Figs. 4 and 5.

In experiments where high energy monochromatic gamma radiation was registered by LaBr detectors [9,12], it was observed that the

full photon energy can be separated from the first escape peak, up to 25 MeV. It gives a characteristic shape of LaBr gamma spectra consisting of a broad continual distribution and a visible peak at the high energy end. Such a structure of spectra was not observed in the measurement of high energy electrons, as can be seen in Figs. 4 and 5. The energy threshold for the creation of an electron–positron pair by electrons is higher and the cross section is lower than in photon interactions. This means that a significantly lower number of pairs is produced by electrons and that the escape process after annihilation does not contribute to the final shape of spectra.

Although not well separated, all the spectra consist of a narrow Gaussian peak that corresponds to events when electrons deliver their complete energy to a scintillator and a long low-energy tail. The continuous structure, which arises from events in which a part of the energy of the electron has escaped detection, is connected to the left side of the Gauss peak. The peak of full energy deposition and its right edge from the rest of distribution was fit by Gauss function. Thus the peak positions were used in order to estimate the energy of incident electrons.

And finally, the calibration graph for BGO, LaBr and plastic detectors is given in Fig. 6. The X axis represents the table energy values of ^{60}Co and the energies of LINAC electron beam in the light of the In-activation method calibration. The Y axis displays the energy E^* of the same radioactive sources and electron beam obtained using initial energy—integral calibration. This means that Y coordinate of points presented in Fig. 6 were determined using mentioned initial calibration. Initial extrapolated calibration is presented by a dashed line at Fig. 6.

Initial calibration of BGO and plastic detector allowed us to get an acceptable energy calibration in a broad energy region using ^{60}Co and ^{137}Cs gamma lines. It can be seen that BGO and plastic detectors calibrations remain linear in the observed energy range of incident electrons. Due to the lack of reliable data concerning a detection of electrons by BGO, LaBr and plastic detectors, our results can be compared with the results of experiments when photons were measured. The dependence between channel number and photon energy was linear when BGO detectors were used in photon detection in the energy region up to 20 MeV [4]. In reference [6] can be seen that an energy response of plastic detectors is linear as well. Considering that no measures for reduction of light output of LaBr detector were taken, obtained energy calibration is non-linear. As can be seen from Fig. 6 the nonlinearity for LaBr can rise up to 30% in the observed interval of electron energies. According to the experimental evidence presented in reference [13], when protons are measured, at higher energies (over 30 MeV) even saturation in energy response can be expected. If the lower phototube voltage is applied [11], dependence between channel number and energy can be linear up to 10 MeV of photon energy. Difference up to 10% appears at 17 MeV. Good linearity of LaBr detectors can be achieved using specifically designed active voltage divider [10]. In this case, 2.7% of deviation was obtained at 22.6 MeV. If the energy signal was derived from one of dinodes, good linearity can be achieved as well [12].

4. Conclusion

It is shown that the ratios of saturation activities can be a very valuable tool for the determination of an unknown bremsstrahlung endpoint energy (and electron energy striking a target) after proper calibration in a well-known bremsstrahlung beam. Natural Indium can be a good choice for an activation detector because several useful products of photon induced reactions can be obtained through isomer excitation and nuclear photo effect. In the energy region of interest (between 11 MeV and 25 MeV) three different ratios of saturation activities can be obtained using measured gamma spectra after activation. It is very important to underline that all three ratios give consistent results when used in the determination of unknown endpoint energy. This means that any of them can be used, depending on the energy region. In

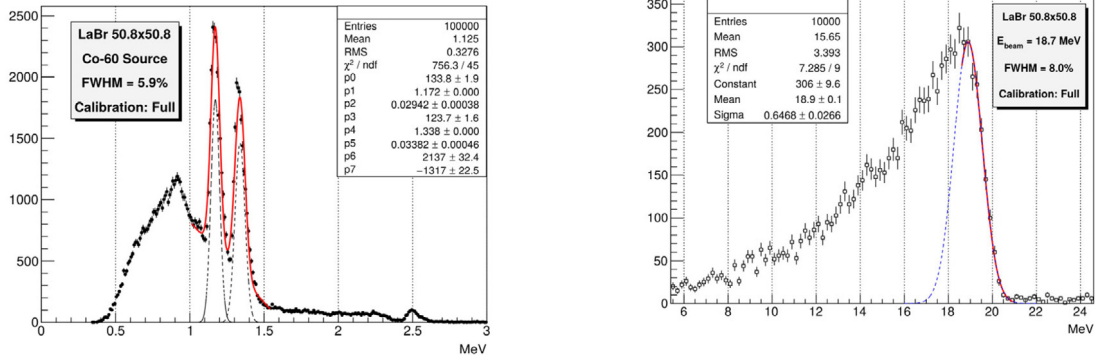


Fig. 4. The spectra of ⁶⁰Co (left) and LINAC-200 accelerator electrons beam energy 18.7 MeV (right), measured by LaBr detector.

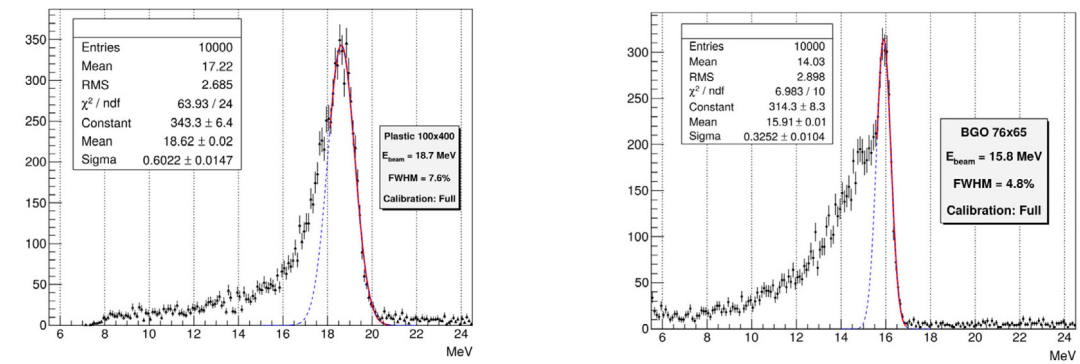


Fig. 5. The spectra of LINAC-200 accelerator electrons, measured by plastic (18.7 MeV) and BGO detector (15.8 MeV).

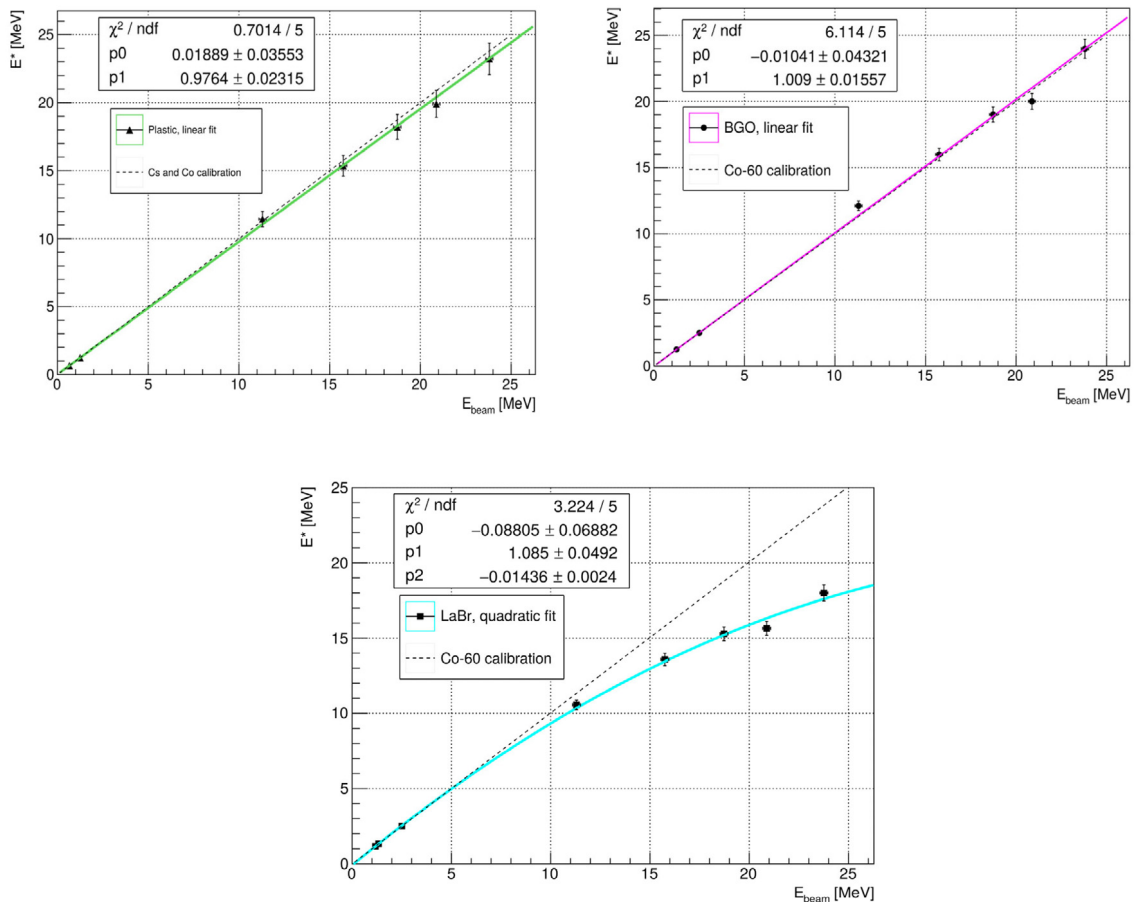


Fig. 6. Linearity of plastic, BGO and LaBr detector response.

the case when all three energy regions overlap, the weighted mean of all three ratios can be used. The $R(^{114\text{m}}\text{In})/R(^{115\text{m}}\text{In})$ ratio can be used in energy region of 10 MeV above. Ratios $R(^{113\text{m}}\text{In})/R(^{115\text{m}}\text{In})$ and $R(^{111}\text{In})/R(^{115\text{m}}\text{In})$ cover similar energy areas. If the experimental conditions are such that it is necessary to perform a fast energy calibration, the ratio $R(^{113\text{m}}\text{In})/R(^{115\text{m}}\text{In})$ has a great advantage due to the much shorter period of the half-life of $^{113\text{m}}\text{In}$ as well as the larger intensity of the relevant gamma line. The shortcoming of the described technique is that it can be used in a limited energy region. This region is determined by the maximal energy of a referent device having a well calibrated energy output (Microtron in our case).

The shapes of spectra obtained in this study are very similar to the shape of high energy photon spectra. Only one small difference appears in the case of LaBr detectors. This is because of a well-known structure at the high energy part, where the full energy peak is separated from the first escape peak. It was not observed when LaBr was exposed by electrons. Preliminary results showed that BGO and plastic detectors have a linear energy calibration in a broad energy range, up to 25 MeV. LaBr detectors do not show linearity. The very same performance was already observed in experiments with high energy photon radiation. Fortunately, this non-linearity is not an inherent property of LaBr crystal. It is rather an outcome of the PMT performances which cannot accept a high light output of LaBr crystal. It was found, in the case of photon detection, that there are mechanisms by which the output of the LaBr detector can be linearized (attenuation of light, removal of signals from lower dynodes). If there is a need for a linear response of LaBr detectors in the detection of high-energy electrons, similar measures can also be taken, with a small loss of the energy resolution.

Acknowledgments

The authors would like to express thanks for V.M. Bystritsky, P. Smolyanskiy, A. Zhemchugov and D. L. Demin for the helpful and discussion during this work.

References

- [1] XFEL: The European X-ray Free-Electron Laser - Technical Design Report, ISBN 3-935702-17-5.
- [2] Heavy ion collider facility NICA at JINR (Dubna) status and development 07 2012 Melbourne, ICHEP-2012.
- [3] H. Vincke, et al., *Nucl. Instrum. Methods A*484 (2002) 102.
- [4] D.L. Demin, Preprint of the JINR, Dubna (2012) E15-2012-107.
- [5] В.М. Быстрицкий и др. Письма в ЭЧАЯ, 2013, т.10, 6(183), с. 925..
- [6] G. Beaudoin, et al., *Nucl. Instrum. Methods A*249 (1986) 379.
- [7] Акимов Ю.К. Фотонные методы регистрации излучений. Дубна: ОИЯИ, 2006.
- [8] G. Gosta, et al., *Nucl. Instrum. Methods A*879 (2018) 92.
- [9] M. Dhibar, et al., *Nucl. Instrum. Methods A*883 (2018) 183.
- [10] A. Giaz, et al., *Nucl. Instrum. Methods A*729 (2013) 910.
- [11] M. Ciemala, et al., *Nucl. Instrum. Methods A*608 (2009) 76.
- [12] I. Mazumdar, et al., *Nucl. Instrum. Methods A*705 (2013) 85.
- [13] F.G.A. Quarati, et al., *Nucl. Instrum. Methods A*629 (2011) 157.
- [14] M. Krmar, et al., *Nucl. Instrum. Methods A*901 (2018) 133.
- [15] С.П.Капица, В.Н.Мелехин Микротрон Издат.Наука Москва 1969 г.
- [16] www.crystals.saint-gobain.com.
- [17] N.V. Vinogradova, et al., *Instrum. Exp. Tech.* 32 (4) (1990) 791.
- [18] ESTAR Stopping power and range tables for electrons, NIST, <http://physics.nist.gov/PhysRefData/Star/Text/ESTAR.html>.